

System reduction strategy for Galerkin models of fluid flows

Bernd R. Noack^{1,*},[†], Michael Schlegel¹, Marek Morzyński² and Gilead Tadmor³

¹*Department of Fluid Dynamics and Engineering Acoustics, Berlin Institute of Technology MB1,
D-10623 Berlin, Germany*

²*Institute of Combustion Engines and Transportation, Poznań University of Technology, PL 60-965 Poznań, Poland*

³*Department of Electrical and Computer Engineering, Northeastern University, Boston, MA 02115, U.S.A.*

SUMMARY

We propose a system reduction strategy for spectral and Galerkin models of incompressible fluid flows. This approach leads to dynamic models of lower order, based on a partition in slow, dominant and fast modes. In the reduced models, slow dynamics are incorporated as non-linear manifold consistent with mean-field theory. Fast dynamics are stochastically treated and can be lumped in eddy-viscosity approaches. The employed interaction models between slow, dominant and fast dynamics respect momentum and energy balance equations in a mathematically rigorous manner—unlike unsteady Reynolds-averaged Navier–Stokes models or Smagorinsky-type reductions of the Navier–Stokes equation. The proposed system reduction strategy is employed to the cylinder wake benchmark. Copyright © 2009 John Wiley & Sons, Ltd.

Received 19 November 2008; Accepted 16 February 2009

KEY WORDS: Galerkin method; system reduction; mean-field model; eddy viscosity; finite-time thermodynamics

1. INTRODUCTION

Focus of this study is a system reduction strategy for Galerkin systems. A large portion of current fluid dynamics research falls in the category of system reduction. The Navier–Stokes equation (NSE) represents a trusted full-scale model for the evolution of fluid flows. The set of permissible velocity fields defines the state space. Knowing the state at one instant allows to predict future states via the NSE. One task of computational fluid dynamics (CFD) consists of finding

*Correspondence to: Bernd R. Noack, Department of Fluid Dynamics and Engineering Acoustics, Berlin Institute of Technology MB1, Straße des 17. Juni 135, D-10623 Berlin, Germany.

[†]E-mail: bernd.r.noack@tu-berlin.de

Contract/grant sponsor: DFG; contract/grant numbers: NO 258/1-1, NO 258/2-3, SCHL 586/1-1, Sfb 557

Contract/grant sponsor: Centre National de la Recherche Scientifique

Contract/grant sponsor: NSF; contract/grant numbers: 0410246, 0524070

Contract/grant sponsor: US AFOSR; contract/grant numbers: FA9550-05-1-0399, FA9550-06-1-0373

a finite-dimensional ‘least-order’ discretization of the velocity field so that sufficiently accurate Navier–Stokes propagators can be constructed. The additional challenge of computing high-*Re* turbulent flows rests on the fact that the discretization of all dynamically relevant scales from large to Kolmogorov scales is not possible. This impossibility leads to necessity of turbulence models for the effect of unresolved scales on the resolved flow. Examples of CFD are large eddy simulation (LES), very large eddy simulation (VLES), detached eddy simulations (DES) and Reynolds-averaged Navier–Stokes (RANS) models. These turbulence models can be interpreted as a dynamic system reduction from a direct numerical simulation (DNS) to a coarser discretization. In spectral methods, the challenge is not the grid but the selection of the expansion modes.

In this study, we address the system reduction problem from a spectral or, more generally, from a Galerkin method perspective. The price is a restricted class of geometrically simple flows. The advantage is the possibility to employ non-linear dynamics systems theory and to ignore spatial inhomogeneities. In short, the modeling problem appears more manageable—an assumption on which many spectral turbulence simulations rest. We restrict ourselves further to system reduction in laminar or transitional flows with fully resolvable degrees of freedom.

Mean-field theory [1] explains the soft onset of flow oscillations and represents a beautiful example of a least-order reduction of the NSE. This theory yields (i) a Galerkin expansion with the three most relevant modes, two oscillatory ones and a mean-field correction; (ii) the mean-field paraboloid slaving the 3D Galerkin space on a 2D manifold; (iii) Landau’s simple amplitude and frequency equations; and (iv) the Reynolds-number dependency of the oscillation. Landau’s (1941) amplitude equation (see, e.g. [2]) and Stuart’s (1958) more general mean-field theory [3] have laid the foundation for center-manifold theory, weakly non-linear models of mode interactions and inertial manifolds [4]. In synergetics [5], the mathematical methods have been adopted and generalized as good recipes for system reduction, including the formulation of the slaving principle.

While mean-field theory describes dynamically a state of large spatial ‘order’, Maxwell’s and Boltzmann’s statistical treatment [6] of molecular chaos can be considered as a highlight result of statistical system reduction. The motion of $\sim 10^{24}$ molecules is parameterized as a maximum entropy state with temperature as the key order parameter. The corresponding kinetic theory for molecular viscosity of gas has inspired Prandtl’s mixing length theory for turbulent shear flows. Later developments of statistical physics took into account various non-equilibrium conditions. One prominent example is finite-time thermodynamics (FTT) [7], which has inspired the authors to a Galerkin system closure. Jaynes (1957) [8] has significantly generalized the entropy concept of statistical physics. Many practical tasks of modern science, like logistics, urban planning, economic planning, signal analysis etc., are rooted on Jaynes’ work [9]. In synergetics [5], Jaynes work has entered as ‘least-biased choice’ of a probability ensemble. Turbulence theory has adopted various concepts of non-equilibrium thermodynamics and statistical mechanics (see, e.g. [10–12]). Currently, mean-field theory and statistical physics approaches have significantly contributed to the understanding of laminar and turbulent flows. Yet, they have hardly affected current turbulence models for CFD.

In the current paper, we propose a systematic strategy to remove and model dynamic degrees of freedoms in Galerkin systems of incompressible fluid flows. In Section 2, a Galerkin model of the cylinder wake is recapitulated. Then, the proposed system reduction strategy is derived from a FTT closure (Section 3). This strategy is applied to the wake model in Section 4. Section 5 describes the limiting behavior of the approach from linear and weakly non-linear dynamics to thermal equilibrium. In Section 6, the main results are summarized and future work is suggested.

2. CYLINDER WAKE MODEL

Here, we outline a Galerkin model for periodic vortex shedding behind a circular cylinder as our benchmark problem. First (Section 2.1), the configuration and direct numerical simulation are described. The simulation data are post-processed in an empirical Galerkin model (Section 2.2). The resulting dynamical system is analyzed and simplified in Section 2.3.

2.1. Numerical simulation

The flow is described in a Cartesian coordinate system x, y , where the origin is in the center of the cylinder, the x -axis is aligned with the flow and the y -axis points in the transverse direction. The location is denoted by $\mathbf{x}=(x, y)$ and the time by t . The dependent variables are the velocity $\mathbf{u}=(u, v)$ and the associated pressure field p . The flow is characterized by the Reynolds number $Re=UD/\nu$ with the cylinder diameter D , the oncoming velocity U and the kinematic viscosity ν . In the following, all quantities are assumed to be non-dimensionalized with D, U , and the fluid density ρ . This implies $\nu=1/Re$.

We consider a circular cylinder in the rectangular computational domain,

$$\Omega=\{(x, y): -5\leq x\leq 15 \text{ and } -5<y<5\}$$

At the inlet and transverse boundaries, the free-stream velocity $(1,0)$ is imposed. At the outflow, a stress-free condition applies. The temporal evolution of the flow is described by the incompressible versions of the mass and momentum balance equations

$$\nabla\cdot\mathbf{u}=0 \tag{1a}$$

$$\partial_t\mathbf{u}+\nabla\cdot(\mathbf{u}\otimes\mathbf{u})=-\nabla p+\nu\Delta\mathbf{u} \tag{1b}$$

The domain is partitioned on an unstructured grid with 31 352 triangles and the evolution equations are solved with a finite-element scheme of third-order accuracy in space and time. Details are described by Morzyński *et al.* [13].

The Reynolds number is set to 100, which is well above the onset of vortex shedding at $Re=47$ [14] and well below the 3D transition around $Re\approx 180$ [15].

2.2. Empirical Galerkin model

We recapitulate a POD model for oscillatory vortex shedding from literature [16]. The unstable steady solution $\mathbf{u}_s(\mathbf{x})$ is chosen as base flow. The fluctuations are resolved with the first eight POD modes of the periodic flow $\mathbf{u}_i, i=1, \dots, 8$. The mean-flow deformation is resolved with a shift mode as ninth mode \mathbf{u}_9 . All nine modes constitute an orthonormal basis and the Galerkin expansion reads

$$\mathbf{u}(\mathbf{x}, t)=\mathbf{u}_s(\mathbf{x})+\sum_{i=1}^N a_i(t)\mathbf{u}_i(\mathbf{x}) \tag{2}$$

Figure 1 illustrates the shift modes, the first two POD modes and their relation to the steady, mean, and periodic flow. The amplitudes of the POD modes occur in pairs of sinusoids shifted by approximately 90° . In particular, the first four pairs describe the first four harmonics of the shedding frequency (see Figure 2).

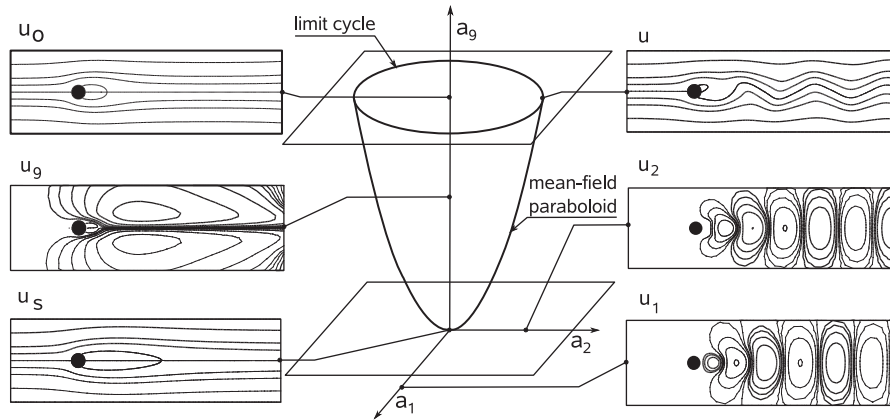


Figure 1. Principal sketch of the Galerkin model for the oscillatory cylinder wake. The mean-field paraboloid characterizes the transients from the steady solution to the periodic solution.

The evolution of the corresponding mode amplitudes $a_i, i = 1, \dots, 9$, is derived from a Galerkin projection onto the Navier–Stokes equation (1b). The resulting autonomous system has constant, linear, and quadratic terms parameterized by c_i, c_{ij} , and c_{ijk} , respectively. Summarizing,

$$\dot{a}_i = c_i + \sum_{j=1}^N c_{ij} a_j + \sum_{j,k=1}^N c_{ijk} a_j a_k \quad (3a)$$

$$0 = c_{ijk} + c_{ikj} + c_{jik} + c_{jki} + c_{kij} + c_{kji} \quad (3b)$$

The last equation expresses an energy conservation property of the non-linear Navier–Stokes term [17].

2.3. Dynamical system

We simplify (3a) to distill important features for the system reduction. First, \mathbf{u}_s in (2) represents a fixed point of the NSE. Hence, the constant term vanishes $c_i = 0, i = 1, \dots, 9$.

Second, the oscillatory nature of the mode amplitudes can be approximated in a Krylov–Bogoliubov ansatz,

$$a_1 + \iota a_2 = A_1 e^{\iota \theta_1}, \quad \theta_1 = \Omega_1 t - \phi_1 \quad (4a)$$

$$a_3 + \iota a_4 = A_2 e^{\iota \theta_2}, \quad \theta_2 = \Omega_2 t - \phi_2 \quad (4b)$$

$$a_5 + \iota a_6 = A_3 e^{\iota \theta_3}, \quad \theta_3 = \Omega_3 t - \phi_3 \quad (4c)$$

$$a_7 + \iota a_8 = A_4 e^{\iota \theta_4}, \quad \theta_4 = \Omega_4 t - \phi_4 \quad (4d)$$

$$a_9 = B \quad (4e)$$

Here, $\iota = \sqrt{-1}$ represents the imaginary unit. The amplitudes A_i , the phases $\phi_i, i = 1, \dots, 4$, and the shift-mode amplitude B are slowly varying functions of time. The frequencies $\Omega_i, i = 1, \dots, 4$ are chosen as harmonics of the shedding frequencies, i.e. $\Omega_i = i \Omega_1, i = 2, 3, 4$.

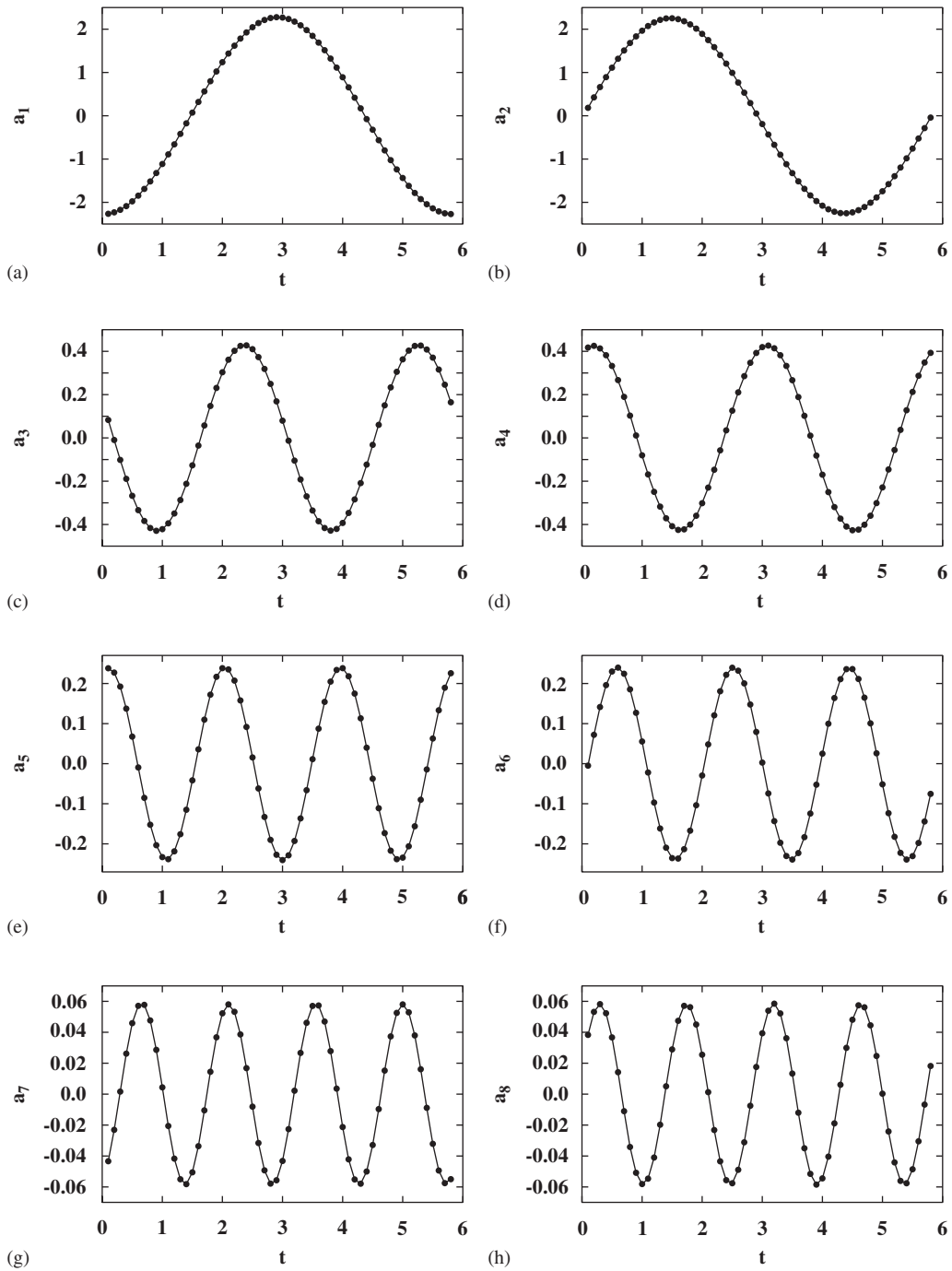


Figure 2. Mode amplitudes a_i , $i = 1, \dots, 8$, of the Navier–Stokes attractor (●—●) over one period.

The Krylov–Bogoliubov ansatz simplifies the linear term of (3)

$$\dot{a}_1 = (\sigma_1 - \beta_1 a_9)a_1 - (\omega_1 + \gamma_1 a_9)a_2 + h_1 \quad (5a)$$

$$\dot{a}_2 = (\sigma_1 - \beta_1 a_9)a_2 + (\omega_1 + \gamma_1 a_9)a_1 + h_2 \quad (5b)$$

$$\dot{a}_3 = (\sigma_2 - \beta_2 a_9)a_3 - (\omega_2 + \gamma_2 a_9)a_4 + h_3 \quad (5c)$$

$$\dot{a}_4 = (\sigma_2 - \beta_2 a_9)a_4 + (\omega_2 + \gamma_2 a_9)a_3 + h_4 \quad (5d)$$

$$\dot{a}_5 = (\sigma_3 - \beta_3 a_9)a_5 - (\omega_3 + \gamma_3 a_9)a_6 + h_5 \quad (5e)$$

$$\dot{a}_6 = (\sigma_3 - \beta_3 a_9)a_6 + (\omega_3 + \gamma_3 a_9)a_5 + h_6 \quad (5f)$$

$$\dot{a}_7 = (\sigma_4 - \beta_4 a_9)a_7 - (\omega_4 + \gamma_4 a_9)a_8 + h_7 \quad (5g)$$

$$\dot{a}_8 = (\sigma_4 - \beta_4 a_9)a_8 + (\omega_4 + \gamma_4 a_9)a_7 + h_8 \quad (5h)$$

$$\dot{a}_9 = (\sigma_\Delta - \beta_\Delta a_9)a_9 + h_\Delta \quad (5i)$$

where

$$h_i := \sum_{j,k=1}^8 c_{ijk} a_j a_k, \quad h_\Delta := \delta_1(a_1^2 + a_2^2) + \delta_2(a_3^2 + a_4^2) + \delta_3(a_5^2 + a_6^2) + \delta_4(a_7^2 + a_8^2)$$

The dynamical system hosts four quadratically coupled oscillators ($i=1, \dots, 8$) with the linear growth rates $\sigma_1 > 0 > \sigma_2 > \sigma_3 > \sigma_4$ and eigenfrequencies $0 < \omega_1 < \omega_2 < \omega_3 < \omega_4$. The system contains also one equation for the slow mean-flow dynamics ($i=9$) with $\sigma_\Delta < 0$. The latter is changed approximately in proportion to the squares of the amplitudes, where δ_i are the gains. The shift-mode amplitude feeds back linearly to the oscillator equations by changing the growth rates and frequencies with interaction parameters β_i and γ_i , $i=1, \dots, 4$. The associated flow physics and the relation to the NSE are described in detail in the literature [16, 18, 19]. In this study, we shall be content with the dynamical systems implications.

Many Galerkin systems of shear flows can be considered as coupled oscillators or have pronounced oscillatory dynamics. Corresponding reduced-order models have been presented for the 2D cylinder wake [20–23], the 3D cylinder wake [24], the 2D and 3D shear layer [25, 26], the transitional and turbulent mixing layer [27, 28], the 2D flow over a cavity [29], the transitional flow over a backward-facing step [30], and the transitional boundary layer [31].

3. SYSTEM REDUCTION STRATEGY

We outline the system reduction strategy. The key enabler is an approximation of an ergodic measure in the Galerkin space. This measure is obtained with the FTT formalism [32] and briefly reviewed in Section 3.1. The FTT equations are employed to model slow and fast modes in Section 3.2.

Finally, Section 3.3 contains practical simplifications of the FTT state variables for the wake model, using the Krylov–Bogoliubov approximation of Section 2.3.

3.1. FTT formalism

Let $\langle \cdot \rangle$ denote an ensemble average. The corresponding Reynolds decomposition for the mode amplitudes reads

$$a_i = m_i + a'_i \quad (6a)$$

$$m_i := \langle a_i \rangle \quad (6b)$$

$$E_i := \frac{1}{2} \langle (a'_i)^2 \rangle \quad (6c)$$

where we introduced m_i for the average and E_i for the modal fluctuation energy. The definition of E_i is permissible since the modes are orthogonal, i.e. the modal energies add up to the total fluctuation energy (TKE).

The constitutive FTT equations for m_i and E_i are obtained from the modal pendants of the Reynolds and TKE equations in the Galerkin space. The unknown second and third moments are expressed in terms of E_i by energetic closure assumptions [32]. The resulting $2N$ equations for $2N$ unknowns read

$$0 = c_i + \sum_{j=1}^N c_{ij} m_j + \sum_{j,k=1}^N c_{ijk} m_j m_k + \sum_{j=1}^N 2c_{ijj} E_j \quad (7a)$$

$$\dot{E}_i = Q_i + T_i, \quad Q_i = q_i E_i, \quad T_i = \sum_{j,k=1}^N T_{ijk} \quad (7b)$$

where

$$q_i = \chi_i + \sum_{j=1}^N \chi_{ij} m_j, \quad \chi_i = c_{ii}, \quad \chi_{ij} = c_{ijj} + c_{iji}$$

$$T_{ijk} = \alpha \chi_{ijk} \sqrt{E_i E_j E_k} \left[1 - \frac{3E_i}{E_i + E_j + E_k} \right]$$

$$\chi_{ijk} := \frac{1}{6} [|c_{ijk}| + |c_{ikj}| + |c_{jik}| + |c_{jki}| + |c_{kji}| + |c_{kij}|]$$

$$0 = \sum_{\substack{i=1 \\ q_i > 0}}^N (Q_i + T_i) \xrightarrow{\text{defines}} \alpha$$

The derivation and discussion of the FTT equations are detailed in the original paper by Noack *et al.* [32]. In the following, we assume the existence of at least one unstable ‘donor’ mode ($q_i > 0$) and at least one stable ‘recipient’ mode ($q_i < 0$). This assumption is fulfilled for the wake model. Numerical experiments suggest to postulate that this assumption is necessary and sufficient for one non-trivial FTT fixed point $[E_1, \dots, E_N] \neq \mathbf{0}$.

The fixed point of (7) corresponds to the steady or the post-transient Navier–Stokes solution. Numerically, the stability properties of the Navier–Stokes solution are observed to transfer to the FTT equations. This is fortunate: Thus, plain forward integration of (7) eventually converges against the non-trivial fixed point associated with the unsteady attractor.

3.2. Decomposition in slow, dominant, and fast dynamics

This section contains the key system reduction elements.

3.2.1. Outline. The constant term of the Galerkin system (3) can be removed by a translation to the fixed point. Under non-degenerate conditions, the linear term can be brought in a simple normal form based on stability eigenmodes. This normal form discriminates clearly stable and unstable subspaces including their temporal behavior (see, e.g. [5, 33]). For short-term transients, strongly damped modes can be neglected. The sole outstanding difficulty of the subject is the assessment of the role of the quadratic non-linear term on the attractor.

As an ansatz, we discriminate modes by their temporal behavior on the attractor. Let A -modes represent the frequency range that shall be resolved in time. Typically, A -modes resolve the coherent structures like von Kármán vortex shedding. Let B -modes have slow dynamics—as compared with the A -modes. Typically, B -modes resolve slow base flow variations. They respond on slowly changing Reynolds stresses due to the A -modes. An example is the shift mode in Figure 1. Let C -modes represent high-frequency dynamics—again as compared with the A -modes. Typically, C -modes are fine-scale structures that act as an energy sink on the coherent structures, i.e. on the A -modes. This translates into the eddy-viscosity model.

We partition all modes in A -, B - and C -modes with indices $i \in \mathcal{I}_A, \mathcal{I}_B$ and \mathcal{I}_C , respectively. In the next step, one type of evolution equations is derived for each group of modes consistent with the constitutive FTT equations (7) and the discussed qualitative properties.

3.2.2. A -modes. The equations for this class of modes read:

$$\dot{a}_i = c_i + \sum_{j=1}^N c_{ij} a_j + \sum_{j,k=1}^N c_{ijk} a_j a_k + \kappa_i (a_i - m_i) \quad (8a)$$

$$\dot{m}_i = \frac{1}{\tau} [a_i - m_i] \quad (8b)$$

$$\dot{E}_i = \frac{1}{\tau} [(a_i - m_i)^2 / 2 - E_i] \quad (8c)$$

Equation (8a) is almost a clone of the Galerkin system (3). The B -modes participate with $a_i = m_i$ on the right-hand side. The C -modes have vanishing a_i but act as an energy sink via the $\kappa_i (a_i - m_i)$ term in agreement with the FTT-modeled transfer term. In other words,

$$2\kappa_i E_i = \sum_{j \vee k \notin \mathcal{I}_A} T_{ijk}$$

Note that this equality defines κ_i as a function of the slowly varying model energy levels $E_i, i = 1, \dots, N$.

Equations (8b) and (8c) estimate the mean values and energy level over a long period τ . These estimates affect the dynamics of the B - and C -modes as described below.

3.2.3. B -modes. The equations for this class of modes read:

$$0 = c_i + \sum_{j=1}^N c_{ij} m_j + \sum_{j,k=1}^N c_{ijk} m_j m_k + \sum_{j=1}^N 2 c_{ijj} E_j \quad (9a)$$

$$m_i = a_i \tag{9b}$$

$$E_i = 0 \tag{9c}$$

The starting point is the Galerkin system (3). The time derivative of m_i on the left-hand side can be neglected due to the assumed slow dynamics. The mean values are shifted by the energy levels of modes A and C . Physically, the energy levels parameterize the modal Reynolds stresses, which change the mean flow [19]. The fluctuation levels of the B -modes have to vanish to ensure consistency with the Reynolds decomposition (6).

3.2.4. *C-modes.* The equations for this class of modes read:

$$\dot{E}_i = Q_i + T_i \tag{10a}$$

$$m_i = 0 \tag{10b}$$

$$a_i = 0 \tag{10c}$$

These modes have vanishing mean and a_i contributions. Their energy is affected by external interactions Q_i and by internal interactions T_i as specified by FTT (7). Often, C -modes are dissipative, and live in balance between welfare (energy from other modes, $T_i > 0$) and dissipation ($Q_i < 0$).

3.2.5. *Properties of the reduced system.* The dynamic degree of freedom (a_i) of a B -mode is slaved to an algebraic equation that contains the (slowly varying) energy levels of the other modes. The C -mode enters only via its energetic effect in the mode interactions. Thus, every B - and C -mode reduces the dynamic degree of freedoms in the dynamical system by one. The interaction between the modes is illustrated in Figure 3.

Note the remarkable symmetry between slow B -modes ($E_i = 0$) and fast C -modes ($m_i = 0$). Within these kinematic constraints for B - and C -modes, Equations (8)–(10), reduce to (7) upon ensemble averaging. Most notably, the interaction terms across different mode classes are consistent

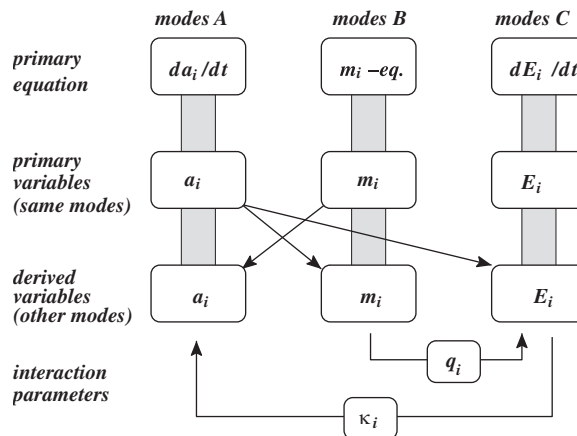


Figure 3. Principal sketch for the dynamic interconnections between A -, B - and C -modes as detailed in Equations (8), (9) and (10), respectively.

with the FTT equations. This implies that the modal momentum and modal energy equations are respected under the given approximations.

3.3. Krylov–Bogoliubov reduction

The Krylov–Bogoliubov ansatz (4) for the wake model allows some simplifications in the state quantities:

$$0 = m_1 = m_2 = \dots = m_8 \quad (11a)$$

$$E_1 = E_2 = \frac{1}{4}(a_1^2 + a_2^2) \quad (11b)$$

$$E_3 = E_4 = \frac{1}{4}(a_3^2 + a_4^2) \quad (11c)$$

$$E_5 = E_6 = \frac{1}{4}(a_5^2 + a_6^2) \quad (11d)$$

$$E_7 = E_8 = \frac{1}{4}(a_7^2 + a_8^2) \quad (11e)$$

$$E_9 = 0 \quad (11f)$$

These equations replace the estimator Equations (8b) and (8c) in our numerical computation. The impact on the fixed point is minimal. But the convergence is much faster.

4. MODELS FOR ATTRACTOR

The system reduction strategy of Section 3 is applied to the wake model of Section 2. First (Section 4.1), the considered systems are described and motivated. In the subsequent Sections 4.2 to 4.5 the corresponding results are presented.

4.1. Considered systems

In the sequel, we consider four systems resulting from the nine-dimensional wake model:

1. SYSTEM A: consists of the Galerkin system. If the Galerkin model was derived from a spectral method, system A would correspond to a DNS.
2. SYSTEM A–B: Here, the POD modes are of class *A* while the shift mode is class *B*. In fluid dynamics, such slaving is rarely pursued in CFD.
3. SYSTEM B–C: Here, the POD modes are stochastically treated (class *C*) while the shift mode remains in class *B*. Thus, only the base flow is resolved. In CFD, this resolution level corresponds to a RANS model.
4. SYSTEM A–B–C: Here, the first two POD modes are dynamically treated (class *A*) while the shift mode is treated algebraically (class *B*) and the remaining modes are statistically modeled (class *C*). Class *C* represents about 5% fluctuation energy in the higher harmonics. In CFD, this resolution level corresponds to an LES.

The mode partitioning of these four systems are illustrated in Figure 4.

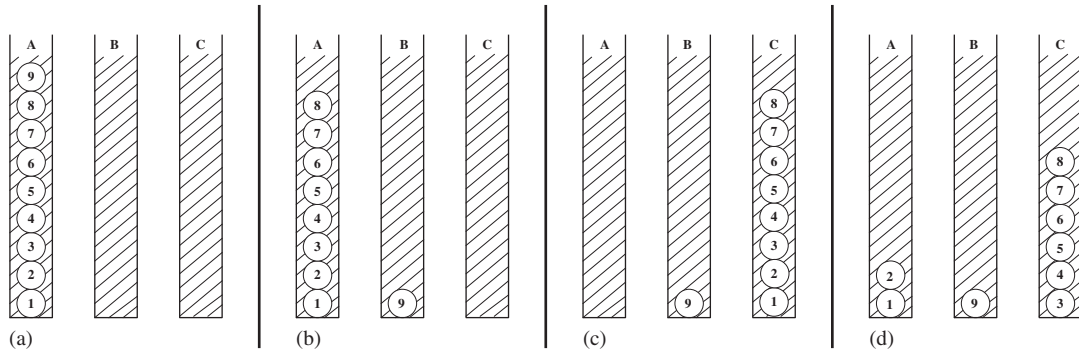


Figure 4. Principal sketch for the considered full and reduced dynamical systems. Modal partitions for (a) system A; (b) system A–B; (c) system B–C; and (d) system A–B–C.

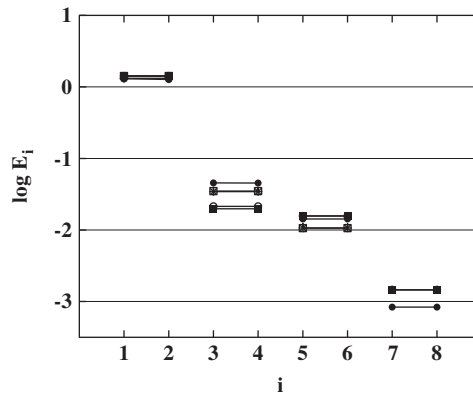


Figure 5. Modal energy distribution E_i , $i = 1, \dots, 8$, of the Navier–Stokes attractor of Figure 2 (●), the Galerkin system (A) (○), system (A–B) (■), system (B–C) (□) and system (A–B–C) (*) as illustrated in Figure 4.

4.2. Dynamic system (A)

The solution of dynamic system (A) is obtained by integrating Equation (3a) until a periodic solution is reached. The mode amplitudes behave like one of the Navier–Stokes attractor displayed in Figure 2. Agreement between Galerkin and Navier–Stokes attractor is within numerical discretization error, i.e. about 1% (see also [16, 20]). The associated energy levels are displayed in Figure 5 as solid circles (Navier–Stokes attractor) and open circles (system A). We shall not pause to discuss small deviations in the higher harmonics representing less than 5% in the total TKE. Instead, we shall be content with a good agreement of the main harmonic contributions from a_1, a_2 .

4.3. Dynamic non-linear manifold system (A–B)

System A–B consists of Equation (8a) for a_i , and Equations (11) for m_i and E_i for $i = 1, \dots, 8$. The B-mode evolution is obtained from Equation (9). The resulting post-transient solution is very

similar to the full system *A*. The associated energy levels are illustrated in Figure 5 as solid squares.

4.4. Stochastic non-linear manifold system (*B–C*)

System *B–C* consists of Equations (9) and (10) with corresponding auxiliary equations. Time integration of that system converges to a fixed point within a dozen periods. The resulting post-transient modal energy distribution is shown in Figure 5 as open squares.

4.5. Deterministic-stochastic non-linear manifold system (*A–B–C*)

Finally, we present a system containing all three kinds of modes. System *A–B–C* consists of Equations (8a), (9)–(11). Thus, the first harmonics is time-resolved in a_1, a_2 while mean-flow and higher harmonics are modeled. Effectively, system *A–B–C* represents a mean-field model with an eddy viscosity for neglected higher harmonics. The post-transient modal energy distribution is indicated by stars in Figure 5. Not accidentally, the distributions of system *B–C* and *A–B–C* coincide well. System *B–C* lumps the oscillator equation for a_1, a_2 of system *A–B–C* by the amplitude equation. This lumping introduces only negligible error due to the numerically observed phase invariance of the oscillator.

5. LIMITING BEHAVIOR

In this section, we discuss limiting behavior of the FTT formalism to elucidate the role of linear and non-linear terms of the Galerkin system. First (Section 5.1), linear dynamics are briefly revisited. In Section 5.2, an amplitude limiting effect of the *B*-mode is highlighted under mean-field assumptions. In Section 5.3, the dissipative effect of low-energy *C*-modes is demonstrated in the thermal equilibrium limit.

5.1. Linear dynamics

Let $\mathbf{a}=\mathbf{0}$ represent an unstable fixed point of the N -dimensional dynamical system (3). Then, $c_1=c_2=\dots=c_N=0$. The linear term of (3) alone will evidently predict the exponential divergence of almost every trajectory, i.e. cannot explain self-amplified, amplitude-limited attractor behavior. A non-linearity is necessary to limit amplitude growth. Two amplitude saturation mechanisms will be discussed in the following two sections.

5.2. Mean-field model

In this section, we consider the oscillatory instability leading to a limit cycle without hysteresis. A least-order Galerkin system describing such a dynamics can be obtained from (5) by neglecting higher harmonics, $a_3=a_4=\dots=a_8=0$ and setting $\beta_\Delta=0$. Such a reduced system describes the limit cycle with about 10% error [16] and reads:

$$\dot{a}_1 = (\sigma_1 - \beta_1 a_9) a_1 - (\omega_1 + \gamma_1 a_9) a_2 \quad (12a)$$

$$\dot{a}_2 = (\sigma_1 - \beta_1 a_9) a_2 + (\omega_1 + \gamma_1 a_9) a_1 \quad (12b)$$

$$\dot{a}_9 = \sigma_\Delta a_9 + \delta_1 (a_1^2 + a_2^2) \quad (12c)$$

Here, $\sigma_1 > 0$ represents the growth rate of the linear stability and ω_1 the corresponding angular frequency. β_1 and γ_1 characterize the effect of the shift mode on the growth rate and frequency, respectively.

In analogy to the B–C system, we consider $i = 1, 2$ as *C*-modes and $i = 9$ as *B*-mode. Then, the corresponding FTT equations are given by

$$\dot{E}_1 = 2\sigma E_1 \tag{13a}$$

$$\dot{E}_2 = 2\sigma E_2 \tag{13b}$$

$$0 = \sigma_\Delta a_9 + 2\delta_1(E_1 + E_2) \tag{13c}$$

where $\sigma = \sigma_1 - \beta_1 a_9$. From (4a), we obtain $A^2/2 = E = 2E_1 = 2E_2$. Thus, Landau’s amplitude equation can easily be derived from (13):

$$\dot{A} = \sigma_1 A - \beta A^3, \quad \beta = \frac{\delta_1 \beta_1}{\sigma_\Delta} \tag{14}$$

This famous equation contains the linear growth rate σ_1 as the driving force behind the oscillation and $-\beta A^3$ as the cubic damping term from the non-linearity.

Mean-field considerations explain how a cubic damping term arises from a dynamic system with quadratic non-linearity. The oscillation creates a Reynolds stress $\propto A^2$, which changes linearly the mean-field deformation a_9 . This deformation changes linearly the effective growth rate thus giving rise to an $\propto A^2 A = A^3$ term. The damping mechanism explains and justifies the inclusion of cubic terms for dynamic systems on more general mean-field manifolds [27, 34].

5.3. Thermal equilibrium

In this section, the role of the quadratic term in the energy cascade will be elucidated. We postulate an energy-preserving dynamic system (3a). This Hamiltonian property requires

$$E = \sum_{i=1}^N E_i = \sum_{i=1}^N a_i^2/2 \equiv \text{const}$$

$$\Leftrightarrow \dot{E} = \sum_{i=1}^N a_i \dot{a}_i = \sum_{i=1}^N c_i a_i + \sum_{i,j=1}^N c_{ij} a_i a_j + \sum_{i,j,k=1}^N c_{ijk} a_i a_j a_k \equiv 0 \quad \forall \mathbf{a} \in \mathcal{R}^N$$

$$\Leftrightarrow \begin{cases} \forall i & c_i = 0 & \text{(I)} \\ \forall i, j & c_{ij} + c_{ji} = 0 & \text{(II)} \\ \forall i, j, k & c_{ijk} + c_{ikj} + c_{jik} + c_{jki} + c_{kij} + c_{kji} = 0 & \text{(III)} \end{cases}$$

Condition (I) and (III) are fulfilled by the assumed fixed point at $\mathbf{a} = \mathbf{0}$ and by the postulated constraint (3b). Condition (II) can be fulfilled by replacing the linear matrix $[c_{ij}]$ with its antisymmetric cousin:

$$[c_{ij}^\circ] = \left[\frac{c_{ij} - c_{ji}}{2} \right]$$

We call this change ‘Hamiltonization’ and the resulting system ‘truncated’.

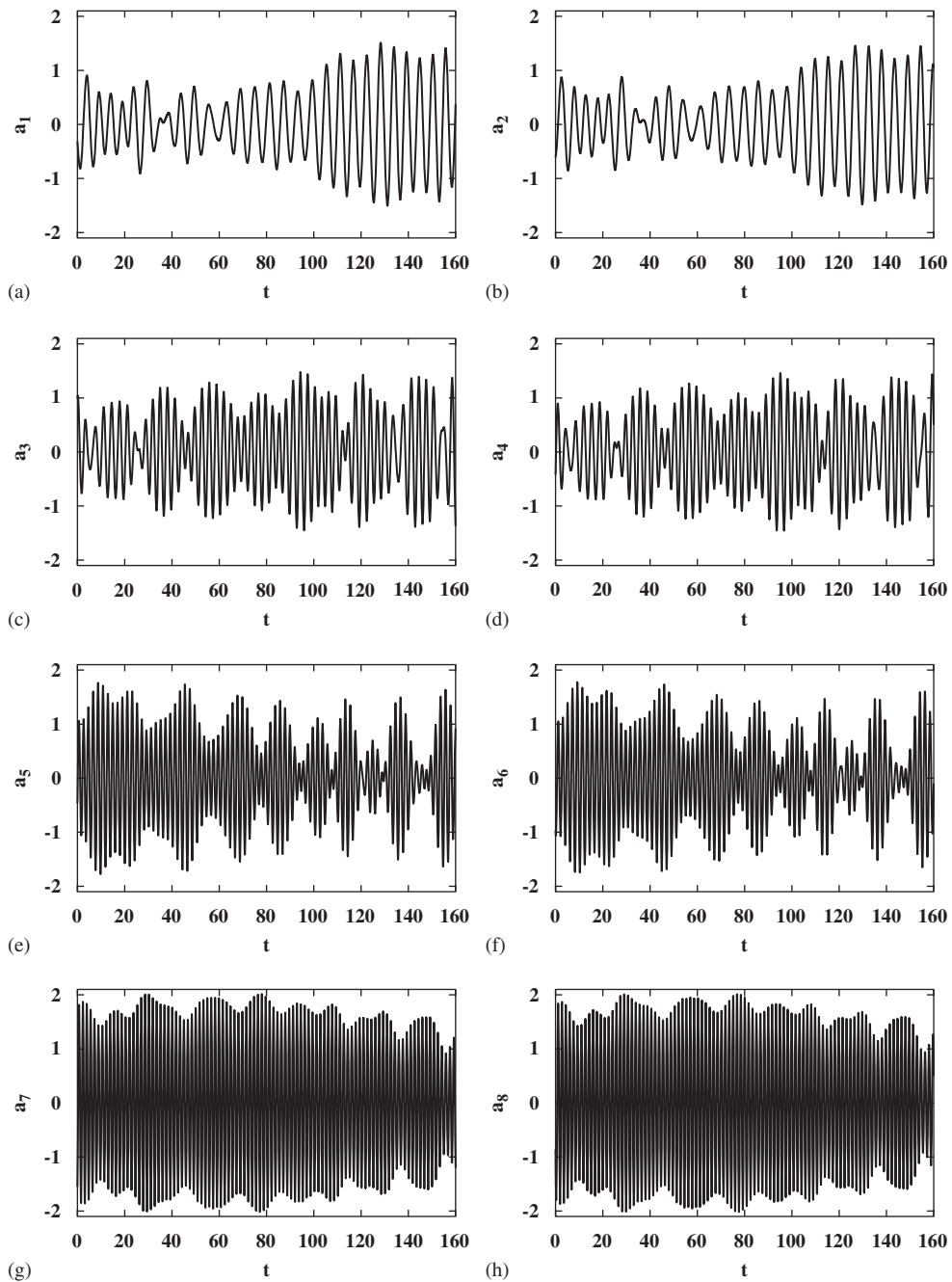


Figure 6. Galerkin system corresponding to Figure 2 with a Hamiltonized linear term. The figure shows the mode amplitudes a_i , $i = 1, \dots, 8$, in a short time window.

In terms of FTT, this modification implies vanishing external interactions, Q_i , or, equivalently, $q_1 = q_2 = \dots = q_N = 0$, as can easily be inferred from (7). Hence, the energy equations read

$$\dot{E}_i = \sum_{j,k=1}^N T_{ijk}, \quad i = 1, 2, \dots, N \quad (15)$$

By construction, energy is an integral of motion from (15):

$$E = \sum_{i=1}^N E_i = \text{const} \quad (16)$$

Moreover, $T_{ijk} \equiv 0$ if $E_i = E_j = E_k$. In particular, the thermal equilibrium

$$E_i = E/N, \quad i = 1, \dots, N \quad (17)$$

solves (15) and (16), i.e. is a fixed point of the FTT equation. If all modes are interconnected, this fixed point is also stable since each triadic interaction T_{ijk} reduces imbalances in energy levels.

Thermal equilibrium is a solution of FTT if the linear term does not introduce energy sources and sinks, i.e. $q_i = 0, i = 1, \dots, N$. The energy cascade from donor modes with large energy from external sources ($q_i > 0$) to recipient modes with lower energy levels and energy sinks ($q_i < 0$) can be considered as an external perturbation of thermal equilibrium. The triadic interactions mitigate the effect of these sources and sinks by establishing a welfare system toward thermal equilibrium. Time scales of energy flow determine the effectiveness of this equilibrium. This is an energetic picture of the eddy-viscosity ansatz.

Next, the thermal equilibrium—predicted by FTT for Hamiltonian systems—is investigated for a numerical solution of the dynamical system. The discussed nine-dimensional wake model is Hamiltonized and its integral of motion (16) is enforced by rescaling to prevent long-term accumulation errors. Figure 6 shows mode amplitudes of Hamiltonized system to be compared with Figure 2. Hamiltonization hardly changes the characteristic frequencies of each mode, but leads to a non-periodic amplitude modulation.

Figure 7 displays the modal energy distribution. Evidently, the FTT-predicted thermal equilibrium is also observed in the truncated Galerkin system. Similar observations have been made for truncated Burger's equations [35] and truncated Euler equations [11].

6. CONCLUSIONS AND OUTLOOK

We have proposed a frame-work for reduction of a dynamic system with energy-preserving quadratic non-linearity. Such dynamic systems arise, for instance, from the traditional Galerkin method or spectral method of incompressible fluid flow. The goal of system reduction is to reduce the dimension of the state space with associated time propagator (dynamics). This implies to eliminate dynamic degrees of freedoms or ordinary differential equations (ODE) by modeling their effect on the remaining dynamical system. The ODEs of slow modes associated with base-flow variations are replaced by algebraic equations defining a manifold in Galerkin space. The ODEs of fast modes associated with fine-scale fluctuations are modeled statistically by their energy distribution. The dynamics of the remaining dominant modes incorporates the effect of the slow and fast modes as inertial manifolds and energy flow terms.

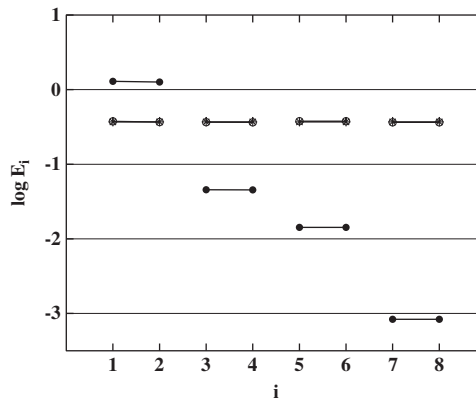


Figure 7. Modal energy distribution E_i , $i = 1, \dots, 8$, of the Navier–Stokes attractor (\bullet), the Galerkin system of Figure 6 (\circ) and the corresponding FTT prediction ($*$). The thermal equilibrium (17) predicted by FTT ($*$) is well obeyed by the Hamiltonized Galerkin system (\circ).

Key enabler for a mathematically rigorous system reduction is a FTT formalism, representing a cumulant closure for the first and second moments. FTT yields approximate versions of the modal Reynolds and TKE equations. FTT allows to derive the interactions between slow, dominant, and fast modes without heuristic assumptions beyond the validated FTT closure. The ensemble averaged equations for slow, dominant, and fast modes including the interaction terms coincide with the FTT equations. For instance, the fast unresolved modes change the inertial manifolds and absorb energy from the dominant modes in a well-defined manner. Furthermore, the slow modes change the dynamics and the energy supplies of the fast modes. In short, FTT offers a design principle for interaction terms across resolved and unresolved flow components.

The proposed system reduction method has been applied to a nine-dimensional empirical wake model. The full system mimics a ‘DNS’, while the considered reduced systems include a RANS-type version with a completely statistical description and an LES-type version with a deterministic resolution of the first harmonics and stochastic model for the higher harmonics. The numerical accuracy of this proof-of-concept study are encouraging.

The proposed FTT-based system reduction accommodates mean-field models, inertial manifolds, a derivation of the eddy-viscosity term and the truncated Euler solution exhibiting thermal equilibrium. Thus, FTT and the proposed system reduction strategy offer a toolkit that reproduces current models of non-linear dynamics and turbulence theory and allows to construct myriad of new models of potential relevance. The authors actively pursue the derivation of an alternative for unsteady RANS and VLES following the sketched path employing physical Galerkin models.

ACKNOWLEDGEMENTS

The authors acknowledge the funding and excellent working conditions of the Collaborative Research Centre (Sfb 557) ‘Control of complex turbulent shear flows’, which is supported by the Deutsche Forschungsgemeinschaft (DFG) and hosted at the Berlin Institute of Technology. The work has been funded by the DFG under grants NO 258/1-1, NO 258/2-3, SCHL 586/1-1 and by the Centre National de la Recherche Scientifique (CNRS). The work of G. Tadmor was partially supported by NSF grants 0410246 and 0524070 and the US AFOSR grants FA9550-05-1-0399 and FA9550-06-1-0373. We are indebted

to the *Bernd R. Noack Cybernetics Foundation*, the *Boye Ahlborn Turbulence Foundation* and Hermine Freienstein-Witt for generous additional resources. We appreciate valuable stimulating discussions with many friends and participants of the 2008 POD workshop in Bordeaux as well as Boye Ahlborn, Rémi Bourguet, and Jose-Eduardo Wesfreid. We thank the local Berlin team as our very stimulating back office: Katarina Aleksic, Hans-Christian Hege, Ingrid Hotz, Jens Kasten, Rudibert King, Oliver Lehmann, Dirk M. Luchtenburg, Nikolas Losse, Mark Pastoor, Jon Scouten, Tino Weinkauff and Olaf Wiederhold. We are grateful for outstanding hardware and software support by Lars Oergel and Martin Franke.

REFERENCES

1. Stuart JT. Nonlinear stability theory. *Annual Review of Fluid Mechanics* 1971; **3**:347–370.
2. Landau LD, Lifshitz EM. *Fluid Mechanics* (2nd edn). Course of Theoretical Physics, vol. 6. Pergamon Press: Oxford, 1987.
3. Stuart JT. On the non-linear mechanics of hydrodynamic stability. *Journal of Fluid Mechanics* 1958; **4**:1–21.
4. Manneville P. *Instabilities, Chaos and Turbulence* (1st edn). Imperial College Press: London, 2004.
5. Haken H. *Synergetics, An Introduction. Nonequilibrium Phase Transitions and Self-Organizations in Physics, Chemistry, and Biology* (3rd edn). Springer: Berlin, 1983.
6. Boltzmann L. Über die Beziehung zwischen dem zweiten Hauptsatze der mechanischen Wärmetheorie und der Wahrscheinlichkeitsrechnung, respektive den Sätzen über das Wärmegleichgewicht (transl.: On the relationship between the second main theorem of mechanical heat theory and the probability theory, respectively with the theorems about the heat equilibrium). *Sitzbericht der Kaiserlichen Akademie der Wissenschaften, mathematisch-naturwissenschaftliche Classe*, Vienna, Austria, 1877; **LXXVI**(Abt. II):373–435.
7. Andresen B. *Finite-Time Thermodynamics* (1st edn). Physics Laboratory II, University of Copenhagen: Copenhagen, 1983.
8. Jaynes ET. Information theory and statistical mechanics. *Physical Review* 1957; **106**:620–630.
9. Kapur JN, Kesavan HK. *Entropy Optimization Principles with Applications* (1st edn). Academic Press: New York, 1992.
10. Ebeling W, Klimontovich YL. *Selforganization and Turbulence in Liquids* (1st edn). BSB B.G. Teubner Verlagsgesellschaft: Leipzig, Germany, 1984.
11. Lesieur M. *Turbulence in Fluids* (2nd edn). Kluwer Academic Publishers: Dordrecht, 1993.
12. McComb DW. *The Physics of Fluid Turbulence* (1st edn). Clarendon Press: Oxford, 1991.
13. Morzyński M, Afanasiev K, Thiele F. Solution of the eigenvalue problems resulting from global non-parallel flow stability analysis. *Computer Methods in Applied Mechanics and Engineering* 1999; **169**:161–176.
14. Williamson CHK. Vortex dynamics in the cylinder wake. *Annual Review of Fluid Mechanics* 1996; **28**:477–539.
15. Zhang H-Q, Fey U, Noack BR, König M, Eckelmann H. On the transition of the cylinder wake. *Physics of Fluids* 1995; **7**:779–795.
16. Noack BR, Afanasiev K, Morzyński M, Tadmor G, Thiele F. A hierarchy of low-dimensional models for the transient and post-transient cylinder wake. *Journal of Fluid Mechanics* 2003; **497**:335–363.
17. Kraichnan RH, Chen S. Is there a statistical mechanics of turbulence? *Physica D* 1989; **37**:160–172.
18. Luchtenburg DM, Günter B, Noack BR, King R, Tadmor G. A generalized mean-field model of the natural and actuated flows around a high-lift configuration. *Journal of Fluid Mechanics* 2009; **623**:283–316.
19. Tadmor G, Lehmann O, Noack BR, Morzyński M. Mean field Galerkin models for the natural and actuated cylinder wake flow. *Physics of Fluids* 2009; submitted.
20. Deane AE, Kevrekidis IG, Karniadakis GE, Orszag SA. Low-dimensional models for complex geometry flows: application to grooved channels and circular cylinders. *Physics of Fluids A* 1991; **3**:2337–2354.
21. Galletti G, Bruneau CH, Zannetti L, Iollo A. Low-order modelling of laminar flow regimes past a confined square cylinder. *Journal of Fluid Mechanics* 2004; **503**:161–170.
22. Bergmann M, Cordier L, Brancher J-P. Optimal rotary control of the cylinder wake using POD reduced order model. *Physics of Fluids* 2005; **17**(097101):1–21.
23. Siegel SG, Seidel J, Fagley C, Luchtenburg DM, Cohen K, McLaughlin T. Low dimensional modelling of a transient cylinder wake using double proper orthogonal decomposition. *Journal of Fluid Mechanics* 2008; **610**:1–42.
24. Ma X, Karniadakis GE. A low-dimensional model for simulating three-dimensional cylinder flow. *Journal of Fluid Mechanics* 2002; **458**:181–190.

25. Noack BR, Papas P, Monkewitz PA. The need for a pressure-term representation in empirical Galerkin models of incompressible shear flows. *Journal of Fluid Mechanics* 2005; **523**:339–365.
26. Wei M, Rowley CW. Low-dimensional models of a temporally evolving free shear layer. *Journal of Fluid Mechanics* 2009; **618**:113–134.
27. Ukeiley L, Cordier L, Manceau R, Delville J, Bonnet JP, Glauser M. Examination of large-scale structures in a turbulent plane mixing layer. Part 2. Dynamical systems model. *Journal of Fluid Mechanics* 2001; **441**:61–108.
28. Noack BR, Pelivan I, Tadmor G, Morzyński M, Comte P. Robust low-dimensional Galerkin models of natural and actuated flows. In *Fourth Aeroacoustics Workshop*, Schröder W, Tröltzsch P (eds). Institut für Akustik und Sprachkommunikation, Technische Universität Dresden, 2004.
29. Samimy M, Debiasi M, Caraballo E, Serrani A, Yuan X, Little J, Myatt J. Feedback control of subsonic cavity flows using reduced-order models. *Journal of Fluid Mechanics* 2007; **579**:315–346.
30. Couplet M, Sagaut P, Basdevant C. Intermodal energy transfers in a proper orthogonal decomposition—Galerkin representation of a turbulent separated flow. *Journal of Fluid Mechanics* 2003; **491**:275–284.
31. Rempfer D. On the structure of dynamical systems describing the evolution of coherent structures in a convective boundary layer. *Physics of Fluids* 1994; **6**:1402–1404.
32. Noack BR, Schlegel M, Ahlborn B, Mutschke G, Morzyński M, Comte P, Tadmor G. A finite-time thermodynamics of unsteady fluid flows. *Journal of Non-Equilibrium Thermodynamics* 2008; **33**(2):103–148.
33. Guckenheimer J, Holmes P. *Nonlinear Oscillations, Dynamical Systems, and Bifurcation of Vector Fields* (corrected 2nd printing). Springer: Berlin, 1986.
34. Aubry N, Holmes P, Lumley JL, Stone E. The dynamics of coherent structures in the wall region of a turbulent boundary layer. *Journal of Fluid Mechanics* 1988; **192**:115–173.
35. Majda AJ, Timofeyev I. Remarkable statistical behavior for truncated Burger-Hopf dynamics. *Proceedings of the National Academy of Sciences of the United States of America* 2000; **97**:12413–12417.